Histidine Oxidation in the S_2 to S_3 Transition Probed by FTIR Difference Spectroscopy in the Ca^{2+}-Depleted Photosystem II: Comparison with Histidine Radicals Generated by UV Irradiation

Catherine Berthomieu*,‡ and Alain Boussac§

CEA Saclay, Service de Bioénergétique (URA CNRS 1290), DBCM, 91191 Gif sur Yvette Cedex, France

Received August 3, 1994; Revised Manuscript Received November 8, 1994⊗

ABSTRACT: FTIR difference and EPR spectroscopies were used to identify the organic radical species formed during the S_2 to S_3 transition in Ca^{2+}-depleted, EGTA-treated, and polypeptide-reconstituted photosystem II membranes (denoted S_2' and S_3', respectively). Ferricyanide was added to the samples to act as an exogenous electron acceptor. Using EPR spectroscopy, it was shown that, under the experimental conditions used, only the species oxidized in the S_3' state was detected during the time required for the acquisition of the FTIR difference spectra. No contributions from the electron acceptor side were observed. The corresponding S_3'/S_2' FTIR difference spectra were recorded at 10 °C in H_2O, D_2O, and with ^{15}N-labeled photosystem II membranes. Spectra were compared with radical-minus-neutral FTIR difference spectra of amino acid model compounds generated by UV irradiation at low temperature. Under our experimental conditions, we did not observe FTIR difference signals consistent with tyrosine oxidation in the S_2' to S_3' transition. The infrared signals characteristic of radical formation with 4-methylimidazole and histidine obtained by UV irradiation of 4-methylimidazolium at pH 6 and of a His-Tyr dipeptide at pH 7 are presented. The analogy found between these spectra and the S_3'/S_2' spectrum obtained *in situ* supports the oxidation of a histidinium in the S_2' to S_3' transition.

Photosystem II (PS II)[1] catalyzes light-driven water oxidation resulting in oxygen evolution. The reaction center of PS II is made up of two membrane-spanning polypeptides (D_1 and D_2) analogous to the L and M subunits of the purple photosynthetic bacterial reaction center [see Michel and Deisenhofer (1988) for a review]. Absorption of a photon leads to a charge separation between chlorophyll molecule(s), designated P_{680}, and a pheophytin molecule. The pheophytin anion transfers the electron to a quinone Q_A, and P_{680}^+ is reduced by a tyrosine residue, Tyr_Z, the tyrosine 161 of the D_1 polypeptide (Barry & Babcock, 1987; Debus et al., 1988b; Metz et al., 1989). A cluster of four Mn located in the reaction center of PS II probably acts both as the active site and as a charge accumulating device of the water-splitting enzyme [see Debus (1992) and Rutherford et al. (1992) for reviews]. During the enzyme cycle, the oxidizing side of PS II goes through five different redox states that are denoted S_n, n varying from 0 to 4 (Kok et al., 1970). The oxygen is released during the S_3 to S_0 transition in which S_4 is a transient state. In addition to Tyr_Z, there is a second redox active tyrosine in PS II, Tyr_D, the tyrosine 160 of the D_2 polypeptide (Barry & Babcock, 1987; Debus et al., 1988a; Vermaas et al., 1988). $Tyr_D^•$ is normally stable in the dark.

Ca^{2+} and Cl^- are two essential cofactors for oxygen evolution [reviewed in Debus (1992)]. The point at which the enzyme cycle is blocked after Ca^{2+} or Cl^- depletion has been shown to be the S_3 to S_0 transition [see Boussac and Rutherford (1994) and Debus (1992) for reviews]. The S_3 state in the inhibited enzyme is denoted S_3' in this paper. The S_3' state is characterized by a split EPR signal centered at $g = 2$ (Boussac et al., 1989, 1992). More data relevant to the understanding of the nature of the Ca^{2+} depletion lesions have been obtained with a chelator-modified preparation. The addition of a range of chelators during or after the salt-washing procedure results in a second modification of the enzyme manifested as a major change of the spectral properties of the S_2 multiline signal and also as the stabilization of the S_2 state [reviewed in Boussac and Rutherford (1994)]. This stable and modified S_2 state is denoted S_2' in this paper.

The S_3' EPR signal was originally interpreted as an organic free radical interacting with the Mn cluster (Boussac et al., 1989). From its UV−visible spectrum, the species was proposed to be a histidine radical (Boussac et al., 1990b). This has been challenged [see, for example, Rutherford and Boussac (1992) and Hoganson and Babcock (1994)], but it was discussed in detail that the experimental evidence favors $His^•$ as the S_3' radical (Rutherford & Boussac, 1992). Recently, we obtained ESEEM data on the S_3' radical and compared them to ESEEM data of imidazole radicals *in vitro*. Although the data were of modest signal-to-noise, it was concluded that they were not inconsistent with an assignment of S_3' to $His^•$ (Zimmermann et al., 1993).

* To whom correspondence should be addressed. Fax: 33-1-69088717.

‡ CEA Saclay.

§ URA CNRS 1290.

⊗ Abstract published in *Advance ACS Abstracts,* January 15, 1995.

[1] Abbreviations: P_{680}, primary electron donor chlorophyll (Chl) of photosystem II (PS II); Tyr_Z, the tyrosine acting as the electron donor to P_{680}; Tyr_D, the tyrosine acting as a side-path electron donor of PS II; Q_A, primary quinone electron acceptor of PS II; Ca-dep. PS II, Ca^{2+}-depleted and EGTA-treated PS II membranes reconstituted with the extrinsic polypeptides; EGTA, ethylene glycol bis(β-aminoethyl ether)-*N,N,N′,N′* tetraacetic acid; PPBQ, phenyl-*para*-benzoquinone; Mes, 2-(*N*-morpholino)ethanesulfonic acid; Im, imidazole; 4-MeIm$^-$, 4-MeImH, 4-MeImH$_2^+$, 4(5)-methylimidazole; His-Tyr, histidine tyrosine dipeptide; EPR, electron paramagnetic resonance; ESEEM, electron spin echo envelope modulation; FTIR, Fourier transform infrared; au, absorbance unit.

0006-2960/95/0434-1541$09.00/0

FTIR difference spectroscopy has been successfully applied to the study of photoinduced reactions in photosynthetic reaction centers and membranes [reviewed by Mäntele (1993a,b)]. With its high reproducibility and good signal-to-noise ratio, it permits the detection of structural changes at the molecular level of all the groups of the protein and cofactors influenced by the electron transfer. In PS II, both the electron acceptor side (Tavitian et al., 1986; Nabedryk et al., 1990; Berthomieu et al., 1990, 1992a; Hienerwadel et al., 1993) and donor side (Berthomieu et al., 1992b; MacDonald et al., 1993; Noguchi et al., 1992a,b, 1993a,b) were investigated. As well, the FTIR difference spectrum corresponding to the S_1 to S_2 transition was published (Noguchi et al., 1992a,b, 1993b).

In this article, the species oxidized in the S_2' to S_3' transition in Ca^{2+}-depleted PS II membranes has been studied by FTIR difference spectroscopy. We have used Ca^{2+}-depleted PS II membranes which were EGTA-treated and where the extrinsic polypeptides were reconstituted after the Ca^{2+}-depletion (denoted Ca-dep. PS II) as described in Boussac et al. (1989). The addition of a mixture of ferricyanide and ferrocyanide ensured both a very fast and complete reoxidation of Q_A^- after the illumination and a fast reduction of the S_3' state into the S_2' state. The successful elimination of the contributions of the electron acceptor side signals resulted in a simplified FTIR difference spectrum where only changes due to the S_2' to S_3' transition are expected to be observed. Spectra were also obtained in D_2O and with ^{15}N-labeled PS II. The histidine oxidation in the S_2' to S_3' transition was probed by comparison with radical-minus-neutral FTIR difference spectra obtained with 4-methylimidazole at pH 6 and with a histidine tyrosine (His-Tyr) dipeptide at pH 7. The radicals formed with the model compounds were obtained by UV photochemistry *in vitro* at low temperature (see also Berthomieu and Boussac, manuscript submitted).

MATERIALS AND METHODS

PS II membranes from spinach chloroplasts were used for the Ca^{2+}-depletion procedure as described in Boussac et al. (1989). ^{15}N-labeled membranes were prepared from spinach grown on a medium supplemented with ^{15}N-labeled minerals [98% as $K^{15}NO_3$, $(^{15}NH_4)_2SO_4$, and $Ca(^{15}NO_3)$, Eurisotop France]. The H_2O/D_2O exchange was done by incubating the membranes overnight in 0.3 M sucrose, 25 mM Mes, pD 6.5, and 10 mM NaCl in D_2O at 8 °C. The buffer in D_2O was prepared by two successive lyophilizations and solubilizations in D_2O of the Ca^{2+}-free medium prepared in H_2O as in Boussac et al. (1989). All the preparations were in Mes buffer at pH 6.5.

Ferricyanide (48 mM) and ferrocyanide (16 mM, final concentrations) were added to the Ca-dep. PS II (≈8 mg Chl/mL), and the membranes were collected by centrifugation (150000*g*, 30 min). For EPR experiments, the pellet was painted on a mylar sheet which was inserted into an EPR quartz tube. After dark adaptation for 10 min at 0 °C, the samples were frozen immediately in liquid nitrogen. Continuous illumination of the samples was done with a 800-W projector lamp through water and infrared filters. The tube was placed in a nonsilvered Dewar filled with ethanol cooled to 0−8 °C with dry ice, and the S3′ signal was generated as in Boussac et al. (1989). After various dark periods following the illumination, the EPR tubes were immersed in the dark in liquid nitrogen. For measurements done at room temperature, the samples were illuminated in the EPR cavity. CW-EPR spectra were recorded at room temperature or at liquid helium temperatures with a Bruker ER 200D X-band spectrometer equipped with an Oxford Instruments cryostat.

The FTIR sample consisted of the membrane pellet squeezed between two CaF_2 windows. The sample was placed in a cryostat, and the temperature was fixed to 10 °C. The 3 s illumination was performed with a 250-W Xenon lamp (Oriel) equipped with red (645 nm) and infrared filters. FTIR spectra were recorded on a Bruker IFS 88 spectrometer equipped with a globar source, a KBr beam splitter, and a MCT-A detector. For each difference spectrum, 64 scans (the recording of which taking 11 s) were recorded before and after the 3 s illumination, and the difference spectrum was then calculated. Difference spectra were averaged from a large number of cycles. The dark period between two consecutive cycles was 1 min. Formation of the radical in the His-Tyr dipeptide (purchased from ICN) and in 4-methylimidazole was done by UV irradiation with a 1000-W Hg/Xe lamp (Oriel) as described in Berthomieu and Boussac (manuscript submitted). The His-Tyr dipeptide was dissolved at a 0.5 M concentration in a 1 M borate buffer at pH 7. FTIR spectra were recorded at 10 K, and 256 scans were taken before and after 16 s of UV irradiation. Spectra obtained with three different samples were averaged.

RESULTS

The light-induced transitions in PS II studied by FTIR difference spectroscopy give absorption changes of $\approx 5 \times 10^{-5}$ to 10^{-3} absorbance units (au) (Tavitian et al., 1986; Berthomieu et al., 1990, 1992a,b; Nabedryk et al., 1990; MacDonald & Barry, 1992; Noguchi et al., 1992a,b, 1993a,b; Hienerwadel et al., 1993; MacDonald et al., 1993). The spectral quality can be improved by averaging the results from a large number of light-induced transitions. Therefore, to allow the averaging of the largest number of spectra, the species formed by the illumination should decay relatively rapidly. Not only the cofactors but also all the protein groups which are modified in the light-induced transition contribute to the FTIR difference spectra. To diminish the complexity of these spectra, conditions should be found where the light-induced transition only involves one cofactor. To study the S_2' to S_3' transition, we have used ferricyanide to eliminate any contribution from the electron acceptor side of PS II. Ferricyanide acts as an exogenous electron acceptor that oxidizes the photoreduced Q_A^-. Ferrocyanide was also added since it reduces S_3' into S_2' (see below). Ferricyanide and ferrocyanide present the advantage of having their infrared modes above 2000 cm^{-1}, i.e., above the absorption region of the protein modes. The concentrations of ferricyanide and ferrocyanide were optimized with regard to the high PS II concentration required in FTIR spectroscopy to overcome the strong absorption of the OH bending mode of water in the mid infrared region.

Figure 1 shows the EPR spectra recorded with the Ca-dep. PS II membranes used in this study. Spectrum a exhibits the stable modified Mn multiline EPR signal recorded in the dark-adapted sample (Boussac et al., 1989). Spectrum a also contains the following features: (1) an intense $Tyr_D^{\bullet}$ signal at ≈3350 G which is suppressed from

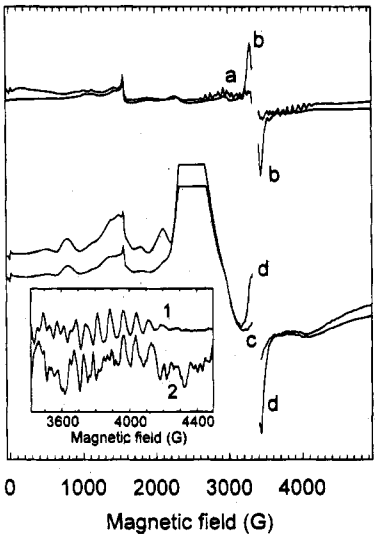

FIGURE 1: Spectra a and b were obtained with Ca-dep. PS II in the presence of 0.5 mM PPBQ, and spectra c and d were obtained with Ca-dep. PS II treated with 48 mM ferricyanide and 16 mM ferrocyanide. Spectra a and c were recorded in dark-adapted membranes (i.e., in the S_2' state). Spectra b and d were recorded after an 8 °C illumination followed by a rapid freezing of the sample (i.e., in the S_3' state). Instrument settings: temperature, 10 K; modulation amplitude, 22 G; microwave power, 20 mW; microwave frequency, 9.4 GHz; modulation frequency, 100 kHz. The central parts of the spectra corresponding to the $Tyr_D^{\bullet}$ region were deleted. The broad signals in spectrum d at ≈800, ≈1500, ≈1800, ≈2100, and ≈4500 G are characteristic of the oxygen signals which often enters in an EPR tube filled with a mylar sheet instead of liquid sample. Spectra in the inset were recorded on a dark-adapted Ca-dep. PS II not painted on mylar sheet without (spectrum 1) or in the presence (spectrum 2) of 48 mM ferricyanide and 16 mM ferrocyanide. A cubic function has been subtracted from both spectra for baseline correction. Spectra recorded on samples with ferricyanide and ferrocyanide were recorded with a gain 50 times smaller and consequently were multiplied by 50 in the figure to be scaled with spectra recorded on samples without ferricyanide.

all spectra shown, (2) the EPR signal from the oxidized Cyt b_{559} which, under the conditions shown, is most evident at its g_z line at ≈2200 G, (3) relatively intense signals at low field arise from contaminating Fe^{3+} ($S = {}^5/_2$) in different environments. Spectrum b was recorded after an 8 °C illumination followed by a rapid freezing (less than 2 s) of the sample and exhibits the split S_3' signal. As was discussed earlier (Zimmermann et al., 1993), the spin quantitation indicates that the S_3' radical corresponds to about one spin per PS II center. Similar spectra were obtained with the ^{15}N-labeled preparation and after the H_2O/D_2O exchange (not shown).

Spectra c and d in Figure 1 were obtained with the Ca-dep. PS II membranes which were treated with 48 mM ferricyanide and 16 mM ferrocyanide and then pelleted by centrifugation. Spectrum c was recorded on dark-adapted membranes. The ferricyanide signal appears as the very intense signal between 2200 and 3000 G. This signal distorted the baseline, and, consequently, the recording of the spectra required a very low signal gain and a high offset on the spectrometer. This resulted in a decrease of the signal-to-noise ratio according to the Bruker spectrometer specifications and made it more difficult to detect the multiline signal. Nevertheless, in the dark-adapted state, the stable S_2' modified multiline signal can still be observed. The inset in Figure 1 compares the modified multiline signals detectable on the same Ca-dep. PS II sample in the absence (spectrum 1) or the presence of ferricyanide/ferrocyanide

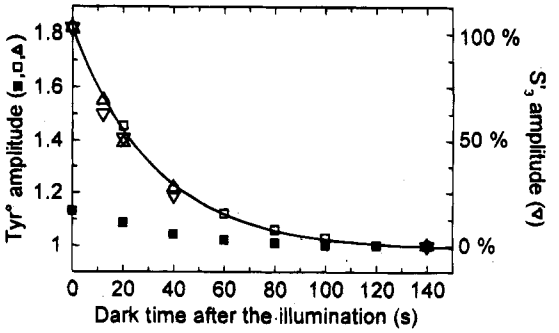

FIGURE 2: Inverted triangles correspond to the amplitude of the S_3' signal which can be induced in Ca-dep. PS II, treated with ferricyanide and ferrocyanide, after an 8 °C illumination (time = 0 s) or after various dark periods at 8 °C before the freezing of the samples. Instrument settings: temperature, 10 K; microwave power, 10 mW; modulation amplitude, 20 G; microwave frequency, 9.4 GHz; modulation frequency, 100 kHz. The right-side-up triangles correspond to the saturation enhancement of the $Tyr^{\bullet}$ signal measured at 50 K with the same sample with which the S_3' signal was measured (inverted triangle). Instrument settings: temperature, 50 K; microwave power, 20 mW; modulation amplitude, 2.8 G; microwave frequency, 9.4 GHz; modulation frequency, 100 kHz. The squares correspond to the amplitude of the $Tyr^{\bullet}$ signal recorded at room temperature with ferricyanide and ferrocyanide and with a microwave power equal to 50 mW (open squares) or equal to 2 μW (closed squares). The $Tyr^{\bullet}$ spectra were recorded first during continuous illumination (time = 0 s). Then one spectrum was recorded in the dark every 20 s. Instrument settings: temperature, 20 °C; modulation amplitude, 2.8 G; microwave frequency, 9.7 GHz; modulation frequency, 100 kHz. The scale for S_3' formation is indicated on the right side of the figure, and the points corresponding to the maximum saturation enhancement effect were normalized to the 100% of S_3' formation.

(spectrum 2) after subtraction of the respective baselines (i.e., using a cubic function). The similar amplitude of the two spectra in the inset indicates that the S_2' state is stable in the sample with 48 mM ferricyanide and 16 mM ferrocyanide. In the presence of 24 mM ferrocyanide alone the S_2' state deactivates into the S_1 state with a half-time of 4 min (not shown). Experiments done with Ca-dep. PS II with 6 mM ferricyanide and 2 mM PPBQ gave the same S_3'/S_2' FTIR difference spectra as those presented below (not shown). With this lower concentration of ferricyanide the EPR multiline signal can be clearly observed. However, in these conditions, the disappearance of the S_3' state in the dark required 40 min, preventing efficient accumulation of the FTIR data.

It has been verified that the S_3' EPR signal could still be light-induced in the presence of the high concentrations of ferricyanide and ferrocyanide used. Illumination at 8 °C of the ferricyanide/ferrocyanide treated sample followed by rapid freezing (less than 2 s) resulted in spectrum d (Figure 1). Spectrum d shows that the S_3' state occurred with similar yield in the absence or in the presence of ferricyanide and ferrocyanide. The small amount of residual multiline signal after the 0 °C illumination can be due to the fast deactivation kinetics of S_3 in these conditions (see Figure 2) and/or to a not totally saturating illumination due to the high concentration of the sample. The width of the S_3' signal (164 G, spectrum d in Figure 1) indicates that the treatment did not induce a release of the extrinsic polypeptides.

With the procedure used to generate the S_3' signal in the presence of ferricyanide and ferrocyanide, the Q_A^- signal could not be detected at 4−5 K (not shown). This shows that ferricyanide has reoxidized Q_A^- within the time required to freeze the sample (less than 2 s). No Chl^+ was trapped

in these conditions. In the Ca-dep. PS II, the ferricyanide/ferrocyanide addition is unable to oxidize the non-heme iron, as indicated by the absence of its characteristic EPR signal [reviewed in Diner et al. (1991b)].

Results related to the stability of the S_3' state at room temperature in the ferricyanide/ferrocyanide treated sample are reported in Figure 2. The half-time of the S_3' state in the presence of ferricyanide and ferrocyanide was monitored by recording the amplitude of the S_3' EPR signal at 10 K (Figure 2, inverted triangles). The samples were illuminated at 0−8 °C and frozen immediately after the illumination (time = 0 s) or after different dark periods at 0−8 °C. The half-time of S_3' was found to be between 20 and 30 s. It has been previously shown that the formation of the S_3' state was accompanied by a saturation enhancement effect on the $Tyr_D^•$ signal at 50 K (Boussac & Rutherford, 1992). Therefore, the $Tyr_D^•$ signal has also been measured here with ferricyanide and ferrocyanide, in the S_2' and S_3' states, in the same sample and with the same saturating microwave power. The amplitude found for the $Tyr_D^•$ signal in the S_3' state was divided by that of the $Tyr_D^•$ signal in the S_2' state and this ratio was normalized as shown in Figure 2 (right-side-up-triangles). The kinetics of the saturation enhancement effect of the $Tyr_D^•$ signal at 50 K also follows that of the S_3' signal in the presence of ferricyanide and ferrocyanide.

The results reported above show that the S_3' state can be light-induced in the Ca-dep. PS II treated with ferricyanide and ferrocyanide. It was shown previously that, in Ca^{2+}- and Cl^--depleted PS II, Tyr_Z could be oxidized at room temperature only in a minority of the centers after formation of the S_3' state (Boussac et al., 1992). To estimate the amount of the light-inducible tyrosine radicals after the ferricyanide/ferrocyanide treatment, the $Tyr^•$ EPR signal was also recorded at room temperature under continuous illumination (time = 0 s) and in the dark at different times after the illumination (Figure 2). The amplitude of the $Tyr^•$ signal was recorded both with high microwave power (50 mW, open squares) and with low microwave power (2 μW, closed squares). Both curves were normalized to the amplitude of the stable $Tyr^•$ EPR signal obtained at 2 μW after a dark period of 140 s. No changes in the amplitude of the $Tyr^•$ signal were observed after 140 s. At high microwave power, the illumination induced almost a doubling (1.8) of the amplitude of the $Tyr^•$ signal. The decay of the $Tyr^•$ signal after the illumination and recorded with a high microwave power matched the kinetics of the decay of the S_3' state. With a microwave power of 2 μW, the signal induced by illumination corresponded to about 10% of the stable $Tyr^•$ signal. The most obvious explanation is that formation of the S_3' signal induced a relaxation enhancement of $Tyr_D^•$, at high microwave power and at room temperature, as already observed at 50 K [Figure 2 right triangle, see also Boussac and Rutherford (1992)]. Four origins may be proposed for the small light-induced signal observed at low microwave power: (1) it corresponds to $Tyr_Z^•$ which may be formed in irreversibly inhibited PS II centers (Boussac et al., 1992); (2) it corresponds to a fast decay of a small proportion of $Tyr_D^•$; (3) it is due to the equilibrium between S_3Z and S_2Z^+; (4) even with a microwave power equal to 2 μW, the $Tyr_D^•$ signal is partially saturated and the formation of the S_3' state is accompanied by a saturation enhancement of the $Tyr_D^•$ signal. To test the latter hypothesis, microwave powers lower than 2 μW should be used, but under these conditions the signal becomes completely undetectable. The fourth hypothesis is favored since (i) it was previously shown that the $Tyr^•$ signal (detected at 50 K) is not increased after formation of S_3' (Boussac & Rutherford, 1992) and (ii) the decay of the $Tyr^•$ signal at low microwave power occurred with a kinetics similar to those at high microwave power. The saturation enhancement effect occurring at room temperature could explain the light-induced $Tyr^•$ EPR signal observed by Dèak et al. (1994) in Cl^--depleted PS II, since they measured it using a microwave power of 20 mW, which is shown here to be saturating. No EPR signal from Chl^+ was detected under continuous illumination at room temperature.

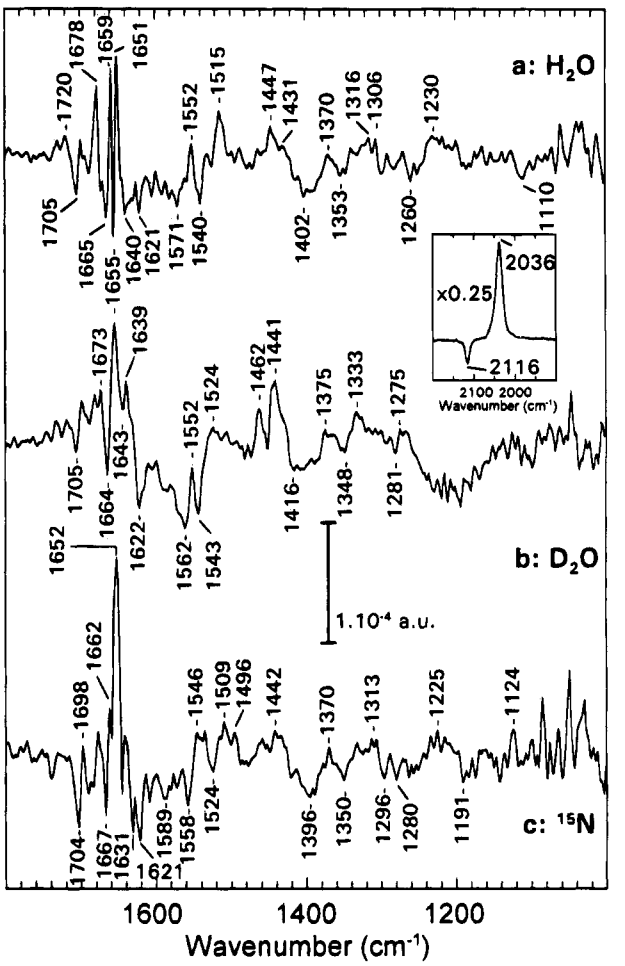

FIGURE 3: S_3'/S_2' FTIR difference spectra obtained with Ca-dep. PS II at 10 °C at pH 6.5 (a) in H_2O, 59 094 scans, (inset) 2200−1900-cm^{-1} region reduced by 4, (b) in D_2O, 49 536 scans, and (c) with ^{15}N-labeled PS II membranes, 50 432 scans, 4 cm^{-1} resolution. All spectra were normalized with their respective ferricyanide/ferrocyanide signal.

In conclusion, the addition of 48 mM ferricyanide and 16 mM ferrocyanide followed by a centrifugation of the membranes results in a pellet in which the S_2' to S_3' transition can be formed in a large fraction of the PS II reaction centers. The reoxidation of Q_A^- occurs in less than 2 s, and the reduction of S_3' into S_2' occurs with a $t_{1/2}$ equal to 20−30 s (curve fitting drawn in Figure 2). Almost no light-induced tyrosine oxidation can be detected.

The FTIR difference spectrum corresponding to the light-induced S_2' to S_3' transition generated at 10 °C and pH 6.5 in Ca-dep. PS II treated with 48 mM ferricyanide and 16 mM ferrocyanide is presented in Figure 3a. In the inset of Figure 3, the region from 2200 to 1900 cm^{-1} is presented, where the ν(CN) stretching modes of ferricyanide and

ferrocyanide absorb at 2116 and 2036 cm^{-1}, respectively. The negative ferricyanide and positive ferrocyanide signals indicate that the reduction of ferricyanide to ferrocyanide is concomitant with the light-induced transition. The typical features of the Q_A^-/Q_A FTIR spectrum are absent in the spectra of Figure 3 (Berthomieu et al., 1990, 1992a). With Tris-treated PS II, it was shown that the presence of high ferricyanide concentrations leads to the oxidation in the dark of a large amount of the non-heme iron (Diner et al., 1991b) which can then be photoreduced. However, no signal observed in the Fe^{2+}/Fe^{3+} FTIR difference spectrum (Hienerwadel et al., 1993) is present in the spectra of Figure 3. The contributions of the electron acceptor side of PS II are eliminated in the presence of ferricyanide and ferrocyanide, and the spectra in Figure 3 are denoted S_3'/S_2'. A baseline recorded in similar conditions with a similar sample but without illumination resulted in a spectrum with maximal absorption changes of 4×10^{-6} au (not shown), indicating that the majority of the signals of Figure 3a are real peaks.

In the 1800−1000 cm^{-1} region, the negative signals correspond to the disappearing S_2' state, whereas the positive ones characterize the S_3' state (Figure 3a). The large number of signals observed indicates that many molecular changes occur besides the expected radical formation. The strongest differential signals are observed at 1665/1659 and 1655/1651 cm^{-1} and most probably reflect contributions from ν(CO) stretching modes of the peptide backbone (amide I mode). The differential signals observed at 1571/1552/1540 cm^{-1} are characteristic of amide II vibrations. A negative signal observed at 1705 cm^{-1} (characteristic of the S_2' state) may be assigned to the ν(C=O) vibration of a protonated carboxylic group either from aspartic or glutamic amino acids or from EGTA. It has been shown that EGTA binding was more rapid in the S_3' than in the S_2' state, suggesting a different mode of binding in the two states (Boussac et al., 1990a). Other negative signals associated with the S_2' state are observed at 1640, 1621, 1571, 1402, 1353, 1260, and 1110 cm^{-1} while the S_3' state is characterized by vibrations at 1515, 1447, 1431, 1370, 1316−1306, and 1230 cm^{-1}. These small signals are reproducibly observed with different samples and are thus significant. They probably arise from amino acid side chains and will be compared to modes observed in the radical-minus-neutral FTIR difference spectra obtained by UV irradiation at low temperature on amino acids and model compounds.

The S_3'/S_2' FTIR difference spectrum obtained with membranes incubated in a D_2O buffer is presented in Figure 3b. The effect of the H_2O/D_2O exchange can help in the discrimination of modes from different amino acid side chains and the assignment of amide I and amide II signals. The 1515 cm^{-1} positive signal observed in Figure 3a is not seen (or downshifted) in D_2O. This is not expected for any mode of a Tyr side chain (Chigadze et al., 1975) and was also not observed for the ν(CO) IR mode assigned at 1513 cm^{-1} for $Tyr^{\bullet}$ (Berthomieu and Boussac, manuscript submitted). Three new positive signals are observed at 1462, 1333, and 1275 cm^{-1} in the S_3'/S_2' spectrum in D_2O (in Figure 3b), while the signals at 1316−1306 cm^{-1} observed in H_2O (Figure 3a) are absent in D_2O. Interpretation of the differences observed in the amide I region is difficult for the moment. In the amide II region, a more negative signal is observed at 1562 cm^{-1} in D_2O than in H_2O, while more positive signals are observed at 1462 and 1441 cm^{-1}. This can be interpreted as a displacement of a positive band from around 1560 cm^{-1} in the S_3'/S_2' spectrum in H_2O (hidden by the overlapping of the negative mode at 1571 cm^{-1}) to 1460−1440 cm^{-1} in D_2O. A shift of ≈100 cm^{-1} upon H_2O/D_2O exchange is characteristic of the amide II (νCN+δNH) mode (Susi, 1969).

The species oxidized in the S_2' to S_3' transition has been proposed to be a histidine (Boussac et al., 1990b). Nevertheless, $Tyr^{\bullet}$ formation has also been discussed (Rutherford & Boussac, 1992; Hoganson & Babcock, 1994). Since isotopic shifts are expected for His and not for Tyr side chains upon ^{15}N-labeling, we studied the S_3'/S_2' difference spectrum obtained with ^{15}N-labeled Ca-dep. PS II (Figure 3c). Small downshifts (3−9 cm^{-1}) are observed on signals at 1640, 1447, 1402, 1353, and 1316 cm^{-1} (Figure 3a) which appear at 1631, 1442, 1396, 1350, and 1313 cm^{-1} in Figure 3c, respectively and which should not correspond to modes of the peptide backbone. The band observed at 1515 cm^{-1} in Figure 3a seems replaced by a positive signal at 1496 and/or 1509 cm^{-1}. This effect indicates that contribution from Tyr side chain is at most a very small part of the 1515-cm^{-1} signal in Figure 3a. The signals at 1571/1552 and 1540 cm^{-1} in Figure 3a are downshifted to 1558/1546 and 1524 cm^{-1} in Figure 3c, in agreement with their assignment to amide II modes, for which a 15-cm^{-1} downshift upon ^{15}N-labeling is expected. The effect of ^{15}N-labeling is also seen at 1660−1650 cm^{-1}. The shifts expected on amide I vibrations are −1 to −2 cm^{-1}. The complexity of this region suggests that more than one or two peptide C=O groups are modified in the S_2' to S_3' transition.

Analysis of signals obtained *in vivo* requires comparisons with model compounds. We recently studied the FTIR and EPR spectra obtained by UV irradiation of aromatic amino acids and of phenol and 4-methylimidazole model compounds (Berthomieu and Boussac, manuscript submitted). The S_3'/S_2' FTIR difference spectrum is compared here with radical-minus-neutral FTIR difference spectra generated on histidine and on 4-methylimidazole. The radical-minus-neutral spectra obtained with phenylalanine or tryptophan (Berthomieu and Boussac, manuscript submitted) are less comparable (see below). With 4-methylimidazole, two different FTIR spectra were obtained at pH 6 and 11. The $His^{\bullet}$/His spectrum was previously generated with His dissolved in a solution containing 28% ammonia (i.e., the final pH was ≈13). At lower pH (i.e., in a borate buffer), the solubility of His is too low to allow the recording of $His^{\bullet}$/His FTIR difference spectra. To generate the $His^{\bullet}$ at pH 7, a His-Tyr dipeptide solubilized in aqueous borate buffer was UV-irradiated at 10 K. At pH 12, a value higher than the p*K* of the tyrosine phenolate group, the UV irradiation of the His-Tyr dipeptide induced a tyrosyl radical as revealed by the characteristic EPR and FTIR spectra (not shown). The radical generated at pH 7 in the dipeptide gives the EPR spectrum displayed in Figure 4 (spectrum a). Its characteristics are very similar to those of the $4\text{-MeImH}^{\bullet+}$ obtained at pH 6 (spectrum b) and $His^{\bullet}$ obtained at pH 6 (spectrum c) and are significantly different from those of $Tyr^{\bullet}$ and of $His^{\bullet}$ and $4\text{-MeIm}^{\bullet}$ obtained at pH 11 (Berthomieu and Boussac, manuscript submitted). At pH 7, Tyr is not oxidized in the His-Tyr dipeptide (or only in a very small proportion, see below) but probably acts as a sensitizer for the oxidation of His by triplet−triplet energy transfer. The yield of $His^{\bullet}$ formation is greatly higher in the dipeptide than in a His solution. Such behavior could be observed by

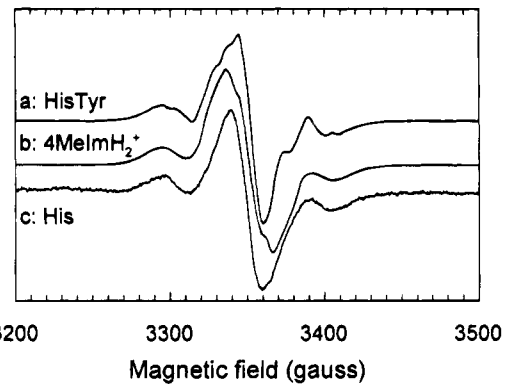

FIGURE 4: EPR spectra of radicals formed by UV irradiation at 77 K in water with 1 M borate buffer: (a) His•-Tyr, pH 7; (b) 4MeIm•, pH 6, and (c) His•, pH 6. Instrument settings: temperature, 20 K; microwave power, 2 μW; modulation amplitude, 2.8 G; microwave frequency, 9.4 GHz; modulation frequency, 100 kHz.

adding micromolar amounts of Tyr in an imidazole (Im) solution at pH 7 (not shown). The addition of tyrosine increased the yield of Im• formation by 3 orders of magnitude. It was shown by Bent and Hayon (1975) that the yield of ^{3}Tyr formation is high between pH 10 and 3, while the yield of radical formation is low in this pH range. It was also shown that triplet quenching can be due to triplet transfer onto another molecule or to the formation of two radicals by electron transfer. Moreover, His is an efficient triplet quenching species (Bent & Hayon, 1975). As no radical pair was observed after UV irradiation at pH 7, it can be concluded that the formation of His• is favored in the His-Tyr dipeptide by triplet transfer from ^{3}Tyr. The use of this dipeptide allowed the formation of His• with high yield at pH 7 and the recording of FTIR spectra.

The FTIR difference spectrum obtained by UV irradiation at 10 K of the His-Tyr dipeptide at pH 7 in H_2O is presented in Figure 5b (thick line) and is denoted His•-Tyr/His-Tyr. This spectrum compares well with the radical-minus-neutral FTIR difference spectrum obtained with 4-methylimidazole in H_2O at pH 6 (4-MeImH$^{\bullet+}$/4-MeImH$_2^+$, Figure 5c), since common signals are observed in Figure 5 spectra b and c at 1432/1433, 1412/1413, 1381/1380, 1348/1341, 1309/1310, and 1083/1082 cm^{-1}. The 1637-cm^{-1} negative signal characteristic of 4-MeImH$_2^+$ (Figure 5c; see Berthomieu and Boussac, manuscript submitted, for the analysis of the 4-MeImH$^{\bullet+}$/4-MeImH$_2^+$ spectra) appears as a small and rather broad band for the dipeptide in Figure 5b, but it could be partially cancelled by superposition with another mode. The similarities in the two spectra allows the assignment of the common signals to the His side-chain modes in Figure 5b and confirms the formation of His• in the His-Tyr dipeptide. This His• obtained at pH 7 with the His-Tyr dipeptide differs from the His• formed at pH $\approx$13 with His (see Berthomieu and Boussac, manuscript submitted). We found that a characteristic IR feature of Tyr• is a band around 2110 cm^{-1} (Berthomieu and Boussac, manuscript submitted). Only a very small signal is observed at 2105 cm^{-1} (with 7 $\times$ 10^{-5} au) in the spectrum obtained with His-Tyr (not shown). The amplitude corresponds to at most 5% of the Tyr• expected if all the His-Tyr had produced a Tyr• with the same yield as the Tyr• obtained from tyrosinate alone. None of the characteristic IR signals of Tyr• in the 1800–1000 cm^{-1} spectral range could be identified in Figure 5b. The negative signal at 1252 cm^{-1} could be due to Tyr (Dollinger et al., 1986), and the differential signal at 1519/1508 cm^{-1} is assigned to a contribution from the ν19a (CC) mode of the Tyr side chain probably influenced by the His• but not involved itself in radical formation.

The signals observed at 1684/1650 and 1579 cm^{-1} in the His•-Tyr/His-Tyr FTIR difference spectrum (Figure 5b) are not found in Figure 5c and do not arise from side chains modes of His and Tyr. We have observed that the amine and carboxylate terminal groups of the amino acids were sensitive to the radical formation (Berthomieu and Boussac, manuscript submitted). In the dipeptide, the carboxylic group of His is involved in the peptide bond with Tyr, and we assign the signal observed at 1684 cm^{-1} to this peptide C=O mode. At 1579 cm^{-1}, large negative signal is due to the COO$^-$ terminal group of the His-Tyr.

The His•-Tyr/His-Tyr spectrum obtained at pD 7 in D_2O is presented in Figure 5b (thin line). The 1684-cm^{-1} signal assigned to the amide C=O is downshifted to 1671 cm^{-1}, suggesting its involvement in hydrogen bonding. The other effects consist of the appearance of new positive signals at 1462, 1330, and 1278 cm^{-1} and the disappearance of the 1381-cm^{-1} signal. This effect of H_2O/D_2O exchange is very analogous to the one observed for the S_3'/S_2' FTIR difference spectra. Positive bands at 1329 and 1280 cm^{-1} were also observed in the 4-MeImD$^{\bullet+}$/4-MeImD$_2^+$ spectrum obtained at pD 6 in D_2O, while the 1310-cm^{-1} signal observed in H_2O (Figure 5c) was also absent in this spectrum (Berthomieu and Boussac, manuscript submitted).

DISCUSSION

To probe the His oxidation in the S_3' state of Ca-dep. PS II, the S_2' to S_3' transition was studied by FTIR difference spectroscopy. The addition of ferricyanide to the Ca-dep. PS II allowed the elimination of the electron acceptor signals to the S_3'/S_2' FTIR difference spectrum. The EPR spectra recorded in the Ca-dep. PS II treated by ferricyanide and ferrocyanide showed that the S_3' state was light-induced in almost all the PS II (Figure 1) and that it was reduced back to the S_2' state with a half-time of 20–30 s (Figure 2). The stability of the S_2' state together with the short time (1 min) between each illumination in the FTIR experiments prevented the deactivation of the S_2' state into the S_1 state and thus a possible contribution from the S_1 to S_2' transition in the FTIR difference spectra. Moreover, it has been shown that the S_1 to S_2 transition is characterized in the FTIR difference spectrum by a narrow and intense negative signal at 1404 cm^{-1} (au $\approx 10^{-4}$; Noguchi et al., 1993b). Using the amplitude of the ferricyanide/ferrocyanide signal, spectrum a in Figure 3 can be scaled to that of the S_1 to S_2 transition reported by Noguchi et al. (1993b). On this scale, the band at 1404 cm^{-1} would have an amplitude of 1.5 $\times$ 10^{-4} au in our spectrum, which is clearly not the case. For all the reasons described above, the spectra in Figure 3 can be considered as characteristic of the species oxidized in the S_2' to S_3' transition in Ca^{2+}-depleted PS II.

The S_3'/S_2' FTIR difference spectrum has been compared with radical-minus-neutral spectra obtained with amino acids and model compounds. The S_3'/S_2' spectrum does not present analogies with the radical-minus-neutral FTIR spectra generated with tryptophan or phenylalanine (Berthomieu and Boussac, manuscript submitted) since the UV-induced Phe•/Phe FTIR spectrum does not exhibit features at $\approx$1260/1230 cm^{-1} which are present in the S_3'/S_2' spectrum. The Trp•/Trp spectrum presents signals at 1456–1446 and 1234 cm^{-1}

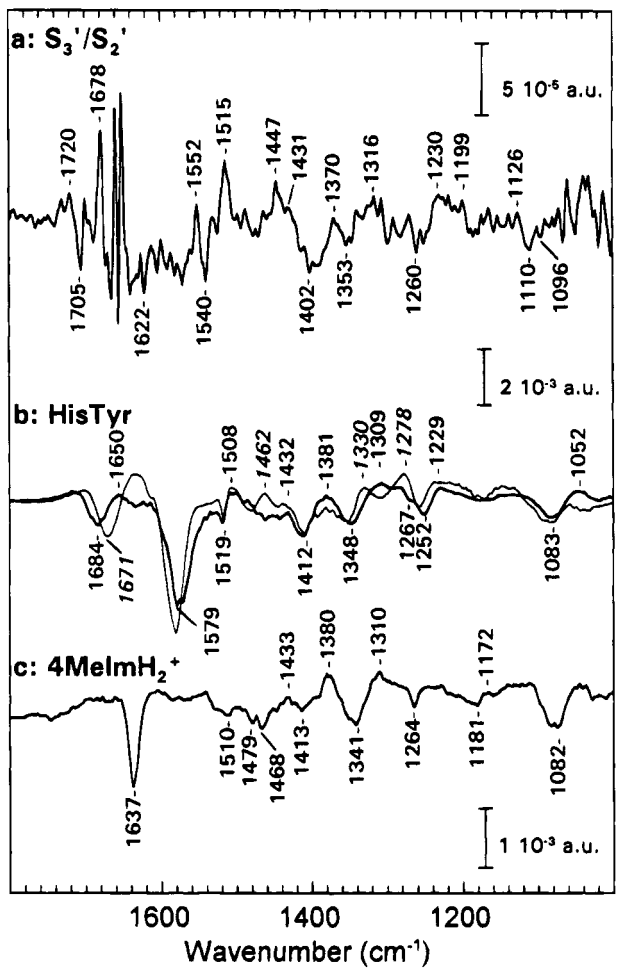

FIGURE 5: (a) S_3'/S_2' FTIR difference spectrum obtained in H_2O at pH 6.5 with Ca-dep. PS II; (b) UV-induced FTIR difference spectra recorded at 10 K of His•-Tyr/His-Tyr at pH 7 in H_2O, thick line, 3840 scans, and at pD 7 in D_2O, thin line, 2560 scans. The frequencies in italics correspond to the sample in D_2O; (c) 4-MeImH•+/4MeImH$_2$+ at pH 6, 5376 scans, 4 cm^{-1} resolution.

that are not observed in the S_3'/S_2' spectrum (Berthomieu and Boussac, manuscript submitted). For these reasons, the possibility that the S_3' radical would be a Phe• or a Trp• is not supported by the FTIR data. The possibility that a Tyr• could be induced in the S_3' state has also been studied. However, we do not find the characteristic and large negative signals at 1268 and 1500 cm^{-1} expected for a tyrosine oxidation. The 1515-cm^{-1} signal observed in the S_3'/S_2' spectrum could possibly be assigned to the Tyr• ν(CO) mode (Berthomieu and Boussac, manuscript submitted). However, this signal is absent or downshifted in D_2O and modified in the spectrum obtained with ^{15}N-labeled membranes, which is not expected for such a Tyr• mode. The analogies are the largest between the S_3'/S_2' spectrum and both the His• formed at pH 7 with the His-Tyr dipeptide and the 4-MeImH•+ formed at pH 6.

The His• radical formed by UV irradiation of the His-Tyr dipeptide at pH 7 is most probably (singly) protonated since it presents signals very close to those of 4-MeImH•+, whereas 4-MeIm• produced at pH 12 exhibits peaks at lower frequencies, i.e., 1425 and 1376 cm^{-1} (Berthomieu and Boussac, manuscript submitted). It is also different from the His• formed at pH $\approx$ 13. We observed a downshift from 1684 to $\approx$1650 cm^{-1} of the absorption frequency of the peptide ν(C=O) mode of the His-Tyr dipeptide upon radical formation. An equivalent effect could be seen upon His• formation *in vivo*, whereas the changes observed at 1580 cm^{-1} in the His•-Tyr/His-Tyr FTIR spectrum are not expected *in vivo*, since they are due to the COO^- terminal group of the His-Tyr dipeptide.

Comparison of the S_3'/S_2' FTIR difference spectrum with the His•-Tyr/His-Tyr FTIR difference spectrum shows a large number of similarities. For example, negative signals at 1402 and 1353 cm^{-1} and positive signals at 1431, 1316−1306, and 1230 cm^{-1} in the S_3'/S_2' spectrum in H_2O are within 10 cm^{-1} for signals observed in the His•-Tyr/His-Tyr spectrum in Figure 5b, thick line. The characteristic overall shape of the two spectra are also very similar. Moreover, the H_2O/D_2O exchange leads to the same effect in the two spectra, with the appearance of signals in D_2O at 1462, 1330, and 1278 cm^{-1} for His•-Tyr and at 1462, 1333, and 1275 cm^{-1} for S_3', while signals observed in H_2O at 1316−1306 cm^{-1} for S_3' and at 1310 for His•-Tyr are not present in D_2O. These similarities strongly suggest that similar events are produced upon the S_2' to S_3' transition *in situ* and upon UV photochemistry of the dipeptide at pH 7. The characteristic 1634 cm^{-1} signal of 4-MeImH$_2^+$ is not clearly observed in the His•-Tyr/His-Tyr difference spectrum. In the S_3'/S_2' spectrum, a negative signal at 1640 cm^{-1}, downshifted in D_2O and possibly downshifted to 1631 cm^{-1} in ^{15}N-labeled PS II (Figure 3), could correspond to this mode. Finally, the negative signal observed at 1110 cm^{-1} in the S_3'/S_2' spectrum is also tentatively assigned to a His side chain mode, since a signal is observed at 1083 cm^{-1} for the dipeptide, at 1107−1088 cm^{-1} for 4-MeImH, and at 1106−1088 cm^{-1} in the His•/His FTIR spectrum (Berthomieu and Boussac, manuscript submitted).

The good correspondence observed between the His•-Tyr/His-Tyr and S_3'/S_2' FTIR difference spectra both in H_2O and in D_2O suggests that in the Ca-dep. PS II, a histidine residue is oxidized in the S_3' state. Moreover, the His• is most probably protonated since the S_3'/S_2' compares better with the model spectra obtained at pH 7 for His• or at pH 6 for 4-MeImH•+ than with the His• and 4-MeIm• obtained at higher pH.

The large number of signals observed in the S_3'/S_2' spectrum are not only assigned to His side chain mode. One differential signal in the amide I region (at 1664/1655 cm^{-1} in D_2O) can probably be assigned to the peptide bond of the His involved in radical formation, as observed for the His-Tyr dipeptide. Ca^{2+} reconstitution and EGTA binding in Ca^{2+}-depleted PS II was shown to be faster in the S_3' state than in the S_2' state (Boussac et al., 1989, 1990a). This was interpreted as a conformational change of the protein between the S_2' and S_3' states. Rearrangement of the protein backbone could explain the sharp signals observed between 1660 and 1640 cm^{-1} and the differential signal observed at 1552/1540 cm^{-1} in the S_3'/S_2' difference spectrum. Finally, a number of signals in the S_3'/S_2' are related to amino acid side chains which change protonation state or environment, at 1705, 1515, and 1447 cm^{-1}. It has been shown that in Ca^{2+} and Cl^- depleted PS II, no proton release occurs during the S_2' to S_3' transition [Boussac et al., 1990b; Lubbers et al., 1994; see also Boussac and Rutherford (1994) for a review]. As we propose that His• formation during this transition is followed by its deprotonation, this suggests that the proton is transferred onto an other group.

It was shown by site-directed mutagenesis on His residues that the two His, D_1 190 and D_1 332, are necessary for the oxygen evolution process in PS II [reviewed in Debus (1992)

and Diner et al. (1991a)]. A His residue was proposed to be oxidized in Mn depleted PS II as a result of the influence of the histidine modifier diethylpyrocarbonate on a thermoluminescence signals (A_T band) associated to the recombination of this His with Q_A^- (Ono & Inoue, 1991, and references therein). The UV spectrum corresponding to the S_2' to S_3' transition in Ca^{2+}-depleted PS II was interpreted in favor of an His$^{\bullet}$ formation by comparison with UV spectra of OH$^{\bullet}$ adduct on histidine (Boussac et al., 1990b). In the present infrared study, the (strong) similarity between the S_3'/S_2' and His$^{\bullet}$-Tyr/His-Tyr FTIR difference spectra both in H_2O and D_2O is also in favor of the oxidation of His in the S_3'-state in Ca^{2+}-depleted PS II.

It was recently shown that His is a ligand of the Mn cluster by specifically labeling PS II membranes with [^{15}N]His (Tang et al., 1994). A similar labeling or a double $^{13}C-^{15}N$ labeling (to increase the IR frequency shifts) of the histidine would be useful for a definitive assignment of the FTIR spectra.

ADDED IN PROOF

A FTIR difference spectrum interpreted as originating from the S_1 to S_2 transition in PS II depleted of Ca^{2+} by citrate treatment has been recently reported (Noghuchi et al., 1995). This spectrum presents similarities with the S_3'/S_2' FTIR spectrum obtained in this work, where control experiments have shown that contributions from S_1 to S_2 are negligible. The apparently higher signal to noise ratio in the work of Noguchi et al. is probably explained by the use of a smoothing procedure.

ACKNOWLEDGMENT

We gratefully acknowledge J. Breton, J.-R. Burie, T. Mattioli, E. Nabedryk, and A. W. Rutherford for discussions and careful reading of the manuscript.

REFERENCES

Barry, B. A., & Babcock, G. T. (1987) *Proc. Natl. Acad. Sci. U.S.A. 84*, 7099−7103.
Baumgarten, M., Philo, J. S., & Dismukes, G. C. (1990) *Biochemistry 29*, 10814−10822.
Bent, D. V., & Hayon, E. J. (1975) *J. Am. Chem. Soc. 97*, 2599−2606.
Berthomieu, C., Nabedryk, E., Mäntele, W., & Breton, J. (1990) *FEBS Lett. 269*, 363−367.
Berthomieu, C., Nabedryk, E., Breton, J., & Boussac, A. (1992a) in *Research in Photosynthesis* (Murata, N., Ed.) Vol. II, pp 53−56, Kluwer Academic Publishing, Dordrecht, The Netherlands.
Berthomieu, C., Boussac, A., Mäntele, W., Breton, J., & Nabedryk, E. (1992b) *Biochemistry 31*, 11460−11471.
Boussac, A., & Rutherford, A. W. (1992) *Biochemistry 31*, 7441−7445.
Boussac, A., & Rutherford, A. W. (1994) *Biochem. Soc. Trans. 22*, 352−358.
Boussac, A., Zimmermann, J.-L., & Rutherford, A. W. (1989) *Biochemistry 28*, 8984−8989.
Boussac, A., Zimmermann, J.-L., & Rutherford, A. W. (1990a) *FEBS Lett. 277*, 69−74.
Boussac, A., Zimmermann, J.-L., Rutherford, A. W., & Lavergne, J. (1990b) *Nature 347*, 303−306.
Boussac, A., Sétif, P., & Rutherford, A. W. (1992) *Biochemistry 31*, 1224−1234.
Chirgadze, Yu. N., Fedorov, O. V., & Trushina, N. P. (1975) *Biopolymers 14*, 679−694.
Dèak, Z., Vass, I., & Styring, S. (1994) *Biochim. Biophys. Acta 1185*, 65−74.
Debus, R. C. (1992) *Biochim. Biophys. Acta 1102*, 269−352.
Debus, R. C., Barry, B. A., Babcock, G. T., & McIntosh, L. (1988a) *Proc. Natl. Acad. Sci. U.S.A. 85*, 427−430.
Debus, R. C., Barry, B. A., Sithole, I., Babcock, G. T., & McIntosh, L. (1988b) *Biochemistry 27*, 9071−9074.
Diner, B. A., Nixon, P. J., & Farchaus, J. W. (1991a) *Curr. Opin. Struct. Biol. 1*, 546−554.
Diner, B. A., Petrouleas, V., & Wendoloski, J. J. (1991b) *Physiol. Plant. 81*, 423−436.
Dollinger, G., Eisenstein, L., & Lin, S.-L. (1986) *Biochemistry 25*, 6524−6533.
Hienerwadel, R., Boussac, A., & Berthomieu, C. (1993) in *Fifth International Conference on the Spectroscopy of Biological Molecules* (Theophanides, T., Anastassopoulou, J., & Fotopoulos, N., Eds.) pp 317−318, Kluwer Academic Publishing, Dordrecht, The Netherlands.
Hoganson, C. W., & Babcock, G. T. (1994) in *Metals Ions in Biological Systems* (Sigel, H., & Sigel, A., Eds.) Vol. 30, pp 77−107, M. Dekker, New York.
Kok, B., Forbush, B., & McGloin, M. (1970) *Photochem. Photobiol. 11*, 457−475.
Lubbers, K., Drevenstedt, W., & Junge, W. (1994) *FEBS Lett. 336*, 304−308.
MacDonald, G. M., & Barry, B. A. (1992) *Biochemistry 31*, 9848−9856.
MacDonald, G. M., Bixby, K. A., & Barry, B. A. (1993) *Proc. Natl. Acad. Sci. U.S.A. 90*, 11024−11028.
Mäntele, W. (1993a) *Trends Biochem. Sci. 18*, 197−202.
Mäntele, W. (1993b) in *The Photosynthetic Reaction Center* (Deisenhofer, J., & Norris, J. R., Eds.) Vol. II, Chapter 10, Academic Press, Inc., New York.
Metz, J. G., Nixon, P. J., Rögner, M., Brudvig, G. W., & Diner, B. A. (1989) *Biochemistry 28*, 6960−6969.
Michel, H., & Deisenhofer, J. (1988) *Biochemistry 27*, 1−7.
Nabedryk, E., Andrianambinintsoa, S., Berger, G., Leonhard, M., Mäntele, W., & Breton, J. (1990) *Biochim. Biophys. Acta 1016*, 49−54.
Noguchi, T., Ono, T., & Inoue, Y. (1992a) *Biochemistry 31*, 5953−5956.
Noguchi, T., Ono, T., & Inoue, Y. (1992b) in *Research in Photosynthesis* (Murata, N., Ed.) Vol. II, pp 309−312, Kluwer Academic Publishing, Dordrecht, The Netherlands.
Noguchi, T., Inoue, Y., & Satoh, K. (1993a) *Biochemistry 32*, 7186−7195.
Noguchi, T., Ono, T.-A., & Inoue, Y. (1993b) *Biochim. Biophys. Acta 1143*, 333−336.
Noghuchi, T., Ono, T., & Inoue, Y. (1995) *Biochim. Biophys. Acta* (in press).
Ono, T., & Inoue, Y. (1991) *Biochemistry 30*, 6183−6188.
Rutherford, A. W., & Boussac, A. (1992) in *Research in Photosynthesis* (Murata, N., Ed.) Vol. II, pp 21−27 Kluwer Academic Publishing, Dordrecht, The Netherlands.
Rutherford, A. W., Zimmermann, J.-L., & Boussac, A. (1992) in *The Photosystems: Structure, Function and Molecular Biology* (Barber, J., Ed.) pp 179−229, Elsevier, New York.
Susi, H. (1969) in *Structure and Stability of Biological Macromolecules* (Tunasheff, S. N., & Fasman, G. D., Eds.) Vol. 2, pp 575−663, Dekker, New York.
Tang, X.-S., Diner, B. A., Larsen, B. S., Lane Gilchrist, M., Jr., Lorigan, G. A., & Britt, R. D. (1994) *Proc. Natl. Acad. Sci U.S.A. 91*, 704−708.
Tavitian, B., Nabedryk, E., Mäntele, W., & Breton, J. (1986) *FEBS Lett. 201*, 151−157.
Vermaas, W. F. J., Rutherford, A. W., & Hansson, Ö (1988) *Proc. Natl. Acad. Sci. U.S.A. 85*, 8477−8481.
Zimmermann, J.-L., Boussac, A., & Rutherford, A. W. (1993) *Biochemistry 32*, 4831−4841.

BI941796F